

## GEOMETRIC MATRIX FOR THIN-WALLED MEMBERS UNDER CONSTANT AXIAL FORCE AND LINEARLY VARIABLE BIAXIAL BENDING AND TWISTING MOMENTS

By Sivaguru KULENDRAN\* and Fumio NISHINO\*\*

This technical note presents a geometric matrix for thin-walled members derived using distribution of linearly varying bending and twisting moments inside an element. The accuracy of the matrix is improved compared with similar matrices derived in the past under the uniform distribution of moments. A numerical example of a simply supported beam is presented in which the critical moments to cause lateral-torsional buckling are compared with the results utilizing the matrix available in literature and the matrix derived in this note to show the better accuracy of the latter.

*Keywords: geometric matrix, thin-walled members, lateral-torsional buckling*

### 1. INTRODUCTION

The stiffness matrices of a thin-walled member subjected to biaxial bending moments, warping moment and axial force are presented in Ref. 1 including geometric matrix. These were calculated on the basis that the various moment distributions within an element are uniform. Accuracy of finite element analysis could be improved by considering moment gradients within an element. In contrast to the geometric matrix, the stiffness matrix corresponding to that of small displacement theory is not altered by this change from uniform to linearly varying distributions of moments. Hence, this technical note presents only the geometric matrix for thin-walled members under the above mentioned general loading condition.

### 2. THEORETICAL DEVELOPMENT

The derivation of the stiffness matrices including the geometric matrix is the same as that of Ref. 1 except for the modifications made with regard to the moment gradients. Stress resultants  $M_y^0$ ,  $M_z^0$ , and  $M_w^0$  are assumed to be constant in the expressions in Eq. 7 of Ref. 1. In the following development the same notations as defined in Ref. 1 are used unless otherwise stated. When linearly varying moment distributions are assumed within an element,  $M''$ 's are replaced by the following expressions

$M_y^0 = M_{y1}^0 + (M_{y2}^0 - M_{y1}^0)x/L$ ,  $M_z^0 = M_{z1}^0 + (M_{z2}^0 - M_{z1}^0)x/L$ ,  $M_w^0 = M_{w1}^0 + (M_{w2}^0 - M_{w1}^0)x/L \cdots (1 \cdot a \sim c)$   
 where the subscripts 1 and 2 denote values at the ends 1 and 2 of an element, respectively.

Substituting Eqs. 4 · b and 6 of Ref. 1, and Eqs. 1 · a ~ c of this note into Eq. 13 of Ref. 1, and

\* M. Eng., Research Associate, Division of Structural Engineering and Construction, Asian Institute of Technology, Bangkok, Thailand.

\*\* Member of JSCE, Ph. D., Professor, Department of Civil Engineering, University of Tokyo, Bunkyo-ku, Tokyo, 113 JAPAN (Formerly, Professor and Vice President for Academic Affairs, Asian Institute of Technology, Bangkok, Thailand).

employing the same interpolation functions for the displacements, the stiffness equation can be obtained in a form similar to that of Eq. 19 of Ref. 1. The terms  $K_{11}$ ,  $K_{22}$  and  $K_{33}$  are identical to Ref. 1, and the terms  $K_{42}$ ,  $K_{43}$  and  $K_{44}$  are changed as follows

$$K_{42} = \int_0^L [N^0 z_s(B')(B')^T + \underline{\{M_{z1}^0 + (M_{z2}^0 - M_{z1}^0)x/L\}(B)(B')^T}] dx \dots\dots\dots (2 \cdot a)$$

$$K_{43} = \int_0^L [-N^0 y_s(B')(B')^T - \underline{\{M_{y1}^0 + (M_{y2}^0 - M_{y1}^0)x/L\}(B)(B')^T}] dx \dots\dots\dots (2 \cdot b)$$

$$K_{44} = \int_0^L [EI_{ww}(B'')(B'')^T + GJ(B')(B')^T + (N^0 r_s^2 + \underline{\{M_{y1}^0 + (M_{y2}^0 - M_{y1}^0)x/L\}\beta_y} + \underline{\{M_{z1}^0 + (M_{z2}^0 - M_{z1}^0)x/L\}\beta_z} + \underline{\{M_{w1}^0 + (M_{w2}^0 - M_{w1}^0)x/L\}\beta_w})(B')(B')^T] dx \dots\dots\dots (2 \cdot c)$$

where the underlined parts are the additional terms appeared due to linearly varying moment distributions. Performing integration on Eqs. 2 · a~c, the modified  $K$ 's can be expressed as

$$K_{42} = \frac{N^0}{L} z_s K_2 + \frac{M_{z1}^0}{L} K_3 + \underline{\{(M_{z2}^0 - M_{z1}^0)/L\} K_4} \dots\dots\dots (3 \cdot a)$$

$$K_{43} = -\frac{N^0}{L} y_s K_2 - \frac{M_{y1}^0}{L} K_3 - \underline{\{(M_{y2}^0 - M_{y1}^0)/L\} K_4} \dots\dots\dots (3 \cdot b)$$

$$K_{44} = \frac{EI_{ww}}{L^3} K_1 + \frac{GJ}{L} K_2 + \left( \frac{N^0}{L} r_s^2 + \frac{M_{y1}^0}{L} \beta_y + \frac{M_{z1}^0}{L} \beta_z + \frac{M_{w1}^0}{L} \beta_w \right) K_2 + \underline{\{(M_{z2}^0 - M_{z1}^0)/L\} \beta_z} + \underline{\{(M_{w2}^0 - M_{w1}^0)/L\} \beta_w} + \underline{\{(M_{y2}^0 - M_{y1}^0)/L\} \beta_y} K_5 \dots\dots\dots (3 \cdot c)$$

where, again the underlined terms are those different from Ref. 1 and the new matrices  $K_4$  and  $K_5$  are given as

$$K_4 = \begin{bmatrix} -1/10 & L/5 & 1/10 & -L/10 \\ 0 & -L^2/30 & 0 & L^2/30 \\ 11/10 & -L/5 & -11/10 & -9L/10 \\ L/10 & 0 & -L/10 & -L^2/10 \end{bmatrix}, \quad K_5 = \begin{bmatrix} 3/5 & -L/10 & -3/5 & 0 \\ -L/10 & L^2/30 & L/10 & -L^2/60 \\ -3/5 & L/10 & 3/5 & 0 \\ 0 & -L^2/60 & 0 & L^2/10 \end{bmatrix} \dots\dots\dots (4 \cdot a, b)$$

### 3. NUMERICAL EXAMPLES

The same example, the simply supported beam as given in Example 1 of Ref. 1, is selected here to show the improvement of accuracy by utilizing the geometric matrix given in this note. Since the geometric matrix of this note and those of Ref. 1 differ only in the terms related to the moments, the difference by the use of these two matrices is more pronounced for members free of axial force. Because of this, only the cases where no axial force is present are considered. The loading conditions and other pertinent information of this example is shown in Fig. 1. To incorporate the effect of moment gradient, the ratio of external moments applied at both ends  $C_1/C_2$ , is changed from  $-1$  to  $+1$  which covers the entire range of moment gradient by selecting,  $C_2$  as the reference moment, and assuming absolute magnitude of  $C_2$  is larger than that of  $C_1$ . The critical moment,  $C_2$ , so selected as for reference moment in the absence of axial force is calculated by performing the eigenvalue analysis.

To check the effectiveness of the matrix of this note, the above defined critical reference moment calculated using both matrices is compared by increasing the number of elements. While using the matrix of Ref. 1, the average value of moments at both ends of an element is taken as the constant moment in the element. Fig. 2 shows the accuracy and convergence of the critical moment with increase in the number of elements obtained using both matrices, the modified matrix and the matrix of Ref. 1. The figure is enlarged in the region where the number of elements exceeds 4 to show the convergence pattern more clearly.

Fig. 2 shows that the modified matrix gives much more accurate results than those of Ref. 1. This significant improvement of accuracy may be due to the fact that only the cases with linearly varying moment distributions are analysed. Nevertheless, a significant improvement of accuracy can be expected for a

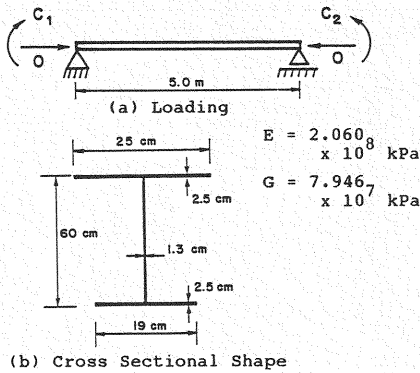


Fig.1 Loading Condition and Cross Sectional Shape.

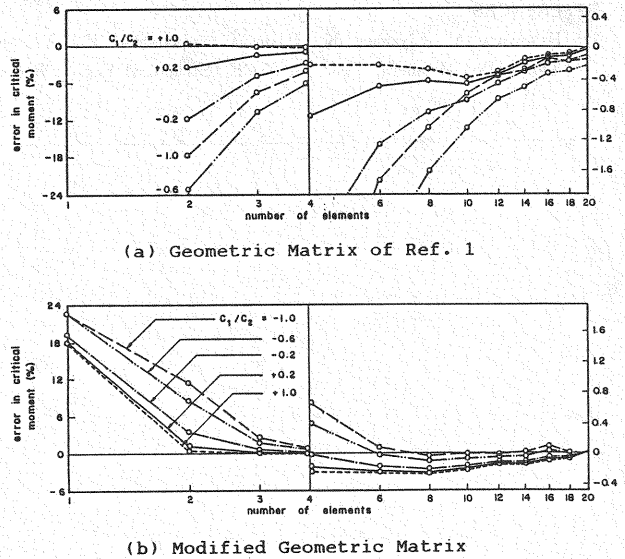


Fig.2 Error Caused by Using Both Matrices versus Number of Elements for Various Combinations of Moment Ratio.

beam with variable moment distributions. With the use of geometric matrix of this note, the percentage error becomes less than 3 % with 3 elements regardless of the ratio of end moments,  $C_1/C_2$ , while the same error is obtained with 8 elements when the geometric matrix of Ref. 1 is used. Using the matrix of Ref. 1, the magnitudes of the percentage error increase steadily for the same number of elements in the negative side when  $C_1/C_2$  moves from  $-1$  approximately to  $-0.6$  reaching the maximum magnitude of error. Then, the error reduces when  $C_1/C_2$  moves towards  $+1.0$  and the curves for  $C_1/C_2=0.6$  and  $C_1/C_2=1.0$  almost coincide with each other. Whereas, the error is positive and largest when  $C_1/C_2$  is equal to  $-1.0$  when the geometric matrix of this note is used with a small number of elements. The use of the proposed matrix and that of Ref. 1 gave identical results when  $C_1/C_2=1.0$  as expected since the moment is constant along the length of the member for this moment distribution. The use of the proposed matrix was found to be particularly advantageous for members with significant variation of bending moment along the length of the element as compared to the use of that of Ref. 1.

Excluding axial forces and boundary conditions which can be incorporated without any difficulty in finite element analysis, the parameters influencing the lateral-torsional buckling moments are  $I_{yy}$ ,  $I_{ww}$ ,  $J$  and  $L$ . Out of these four parameters, one parameter can be eliminated by using it to nondimensionalise the other parameters. Because of this, calculations are also made with various combinations of the values of  $L^4/I_{yy}$ ,  $L^4/J$  and  $L^6/I_{ww}$  and for other boundary conditions such as continuous beams. It is found that the errors for a variety of combinations of these parameters varied from approximately 6 % and 1 % when the number of elements exceeds 4 and 20 elements, respectively, in the method of Ref. 1, while the errors are less than 3 % and 1 % in the proposed method even with as few as 3 and 4 elements, respectively.

#### 4. SUMMARY AND CONCLUSIONS

Based on the theory developed in Ref. 1, modification is made to incorporate linearly varying moment distributions in an element, and the resulting geometric matrix is obtained and presented in explicit form. Numerical examples are worked out and compared with the results using the matrix derived in Ref. 1. This modification is found to result in much more accurate results for the same number of elements when the moment gradient is linear. Improvement of accuracy is expected for the cases of nonlinearly varying moment gradient as well.

REFERENCES

1) Hasegawa, A., Liyanage, K., Ikeda, T. and Nishino, F. : A Concise and Explicit Formulation of Out-of-Plane Instability of Thin-walled Members, Proc. of JSCE, Structural Eng. / Earthquake Eng., Vol.2, No.1, pp.81~89, April 1985.

(Received August 27 1986)